

High-Frequency Photodiode Characterization using a Filtered Intensity Noise Technique

**Doug Baney, Wayne Sorin, Steve Newton
Instruments and Photonics Laboratory
HPL-94-46
May, 1994**

**photodiode, EDFA,
spontaneous
emission, intensity
noise, optical fiber,
ASE, responsivity**

Optical filtering of amplified spontaneous emission improves measurement dynamic range for frequency response measurements of optoelectronic receivers. For high bandwidth receivers, a novel etalon filtered intensity noise technique is proposed. Response measurements using these techniques on a 3 GHz and 30 GHz receiver are demonstrated.



I. Introduction

High-frequency characterization of photodiodes and optoelectronic receivers is important for optical communications and instrumentation as optical receiver bandwidths continually increase. A number of methods have successfully demonstrated high-frequency response measurements beyond 20 GHz. These include time domain picosecond pulse techniques [1], optical heterodyne using two narrow-linewidth tunable laser sources [2] and the optical intensity noise technique [3]. The intensity noise technique is of particular interest given its simplicity. It relies on the generation and subsequent detection of spontaneous-spontaneous (sp-sp) intensity beat noise with a setup consisting of an optical amplifier, the photoreceiver to be characterized and a high frequency electrical spectrum analyzer. The frequency response is found from a measurement of the photocurrent power spectrum which would be flat for a perfect photoreceiver. With this straightforward setup, optical receiver measurements extending well into the millimeter wave frequency range can be performed. Eichen et al. have demonstrated photoreceiver measurements to 22 GHz using the sp-sp intensity beat noise from semiconductor optical amplifiers and have suggested using an erbium-doped fiber amplifier (EDFA) to help overcome the relaxation resonance problems associated with the semiconductor amplifier [3],[4]. An advantage of the intensity noise technique is that the optical intensity fluctuations exist simultaneously at all frequencies, allowing for quick measurement of the photodiode response. Additionally, the low optical polarization dependence, and short source coherence length permit very stable measurements.

The relative intensity noise, RIN, serves as a figure of merit for optical intensity noise sources. It describes the ratio at detection of the photocurrent variance to the square average photocurrent. The average photocurrent is an important parameter in view of the effects of saturation on the photodiode frequency response [5]. The photocurrent

variance determines the measurement dynamic range, which is the difference between the spontaneous-spontaneous beat noise and the combined receiver thermal and shot noise. Thermal noise can be a significant factor limiting measurement dynamic range. Due to losses in the electronic mixing process, an electrical spectrum analyzer noise floor (-143 dBm/Hz @ 30 GHz) is substantially greater than the thermal noise (-174 dBm/Hz) of a 50Ω resistor. A 1 mW optical source ($\lambda_o = 1.55 \mu\text{m}$) with a 30 nm bandwidth induces approximately -139 dBm/Hz photocurrent noise power in a perfect photodiode leaving a measurement dynamic range of 4 dB. Unless higher average optical power is permitted, or a broadband amplitude calibrated preamplifier is available, frequency response measurements of low gain photoreceivers with the conventional intensity noise method can be corrupted by thermal noise. In this letter, we propose and demonstrate methods that provide for significant increases of the optical source RIN, and hence an increase of the measurement dynamic range for frequency response characterization of photoreceivers.

II. Optical Bandwidth Reduction Technique

When unpolarized spontaneous emission with optical bandwidth B_o is detected, a spontaneous-spontaneous (sp-sp) beat noise is generated in bandwidth B_e [3]:

$$\langle \Delta i_{sp-sp}^2 \rangle = 4 R^2(f) \rho_{ASE}^2 B_o B_e \quad (1)$$

Where $R(f)$ is the desired photodiode responsivity and the power spectral density of the optical field is designated by ρ_{ASE} . Frequencies f , are assumed to be much smaller than the optical bandwidth ($B_o \sim 1000 \text{ GHz}$) For simplicity the optical field spectrum was assumed rectangular and the DC responsivity was taken to be unity. As discussed earlier, in view of maximum incident power limitations for photoreceivers, the source RIN is the figure of merit of interest[3]:

$$RIN_{sp-sp} = \frac{\langle \Delta i_{sp-sp}^2 \rangle}{\langle i_{DC} \rangle^2} = R^2(f) \times \frac{1}{B_o} \quad (2)$$

It is apparent from (2) that a reduction of the optical source bandwidth increases the low-frequency RIN. Therefore, for fixed average optical power, post-filtering the ASE source provides a simple way to improve the measurement dynamic range by a factor equal to the ratio of the unfiltered bandwidth to the filtered bandwidth. This provides for a very useful method for characterization of photoreceivers and is shown conceptually in the inset of Figure 1. For high-frequency photodiode characterization, the assumption of a flat RIN spectrum must be carefully examined. Figure 1 shows the effect of bandwidth B_o on the flatness of photodetector responsivity (R) measurement. Data were taken with a monochromator to filter ASE from a superfluorescent source and post amplifying with a second EDFA. Measurements were taken to 10 GHz, above which, background beat noise from the post amplifier begins to mask the measurement for 0.1 nm filter bandwidth. Theory corresponding to a rectangularly filtered ASE source is plotted along with the slope data from the experiment[6]. The theory and experimental data agree very closely, which is indicative of the rectangular passband of the monochromator. This filtered technique was used to characterize a 3 GHz photoreceiver. Figure 2 shows response measurements for a 1 nm filter bandwidth and -7 dBm average optical power, and 1.3 μ m optical heterodyne measurements for comparison. The technique shows excellent agreement when compared with the heterodyne method.

III Etalon-Filtered Technique

While the technique discussed in the previous section provides a significant increase in RIN, reduction of filter bandwidth is limited to the point where roll-off in the RIN spectrum as shown in Figure 1 poses dynamic range limitations. This is particularly true

for high-frequency photoreceivers with performance beyond 20 GHz. Additionally, unamplified photoreceivers require even higher levels of RIN to make satisfactory measurements. It is therefore desirable to increase the RIN as discussed above but at the same time without reducing the high frequency measurement capability. This is accomplished with the second method shown conceptually in Figure 3. The optical source spontaneous emission is filtered by a high finesse, small free spectral range (FSR), Fabry-Perot filter. This results in a spectrum composed of a series of equal height Lorentzian shaped lines extending over tens of nanometers. The filtered sp-sp beat noise RIN, is composed of a series of periodic peaks:

$$RIN = R^2(f) \times \frac{1}{B_o} \times \frac{F}{\pi} \times \sum_{k=0}^{B_o/FSR} \frac{1}{1 + \left(\frac{f - k \cdot FSR}{\Delta\nu} \right)^2} \quad (3)$$

Comparing (2) and (3) it is apparent that this new technique provides a dynamic range improvement of F/π when measurements are performed at the peaks. The high-frequency measurement capability is retained since the optical bandwidth B_o is the same in both techniques. The measurement is no longer continuous with frequency but consists of many sample points separated by the filter FSR.

In the experiment, an EDFA superfluorescent source provided ASE at a 1.55 μm wavelength. A fiber Fabry-Perot filter, with a finesse and a free spectral range of 80 and 680 MHz respectively, filtered the source. This reduced the average power to approximately 27 μW . An EDFA increased the average power to several milliwatts. Fusion splices between the superfluorescent source, the filter and the post-amplifier were used to minimize amplitude ripple from parasitic resonators. A 50 GHz electrical spectrum analyzer displayed the photocurrent power spectrum. The measured frequency

response of a high-speed optical receiver is shown in Figure 4. The receiver consisted of a 14 μm diameter PIN photodiode followed by a traveling wave microwave GaAs amplifier. Measurements were performed three different ways: the unfiltered intensity noise technique, the new Fabry-Perot filtered intensity noise technique and the optical heterodyne technique. The average optical powers for the two intensity noise techniques were equal. Comparing the intensity noise techniques, the new technique offers much improved dynamic range, approximately 17 dB in this case. The improvement over the theoretical expectation of 14 dB maybe due to bandwidth contraction of the superfluorescent source which was driven into saturation to maximize ASE power to the etalon filter. Agreement between the three measurements is good.

IV Discussion and Summary

The new filtered noise techniques has demonstrated a significant improvement in dynamic range over the conventional unfiltered intensity noise techniques for frequency response measurements of optoelectronic receivers. Using this technique to characterize the frequency response of a 30 GHz photoreceiver, a 17 dB dynamic range improvement was demonstrated. The optical arrangement for this technique is slightly more complex than the unfiltered technique, but it is still simpler than with heterodyne techniques which require continuously-tuned single frequency narrow linewidth lasers with polarization preserving optics. The improved dynamic range allows for the possibility of measuring the frequency response of photodiodes using an electrical spectrum analyzer as a receiver with no intervening electrical preamplifier. A further increase in dynamic range is achieved by a combination of the two filtered techniques described.

Acknowledgments

The authors thank Mr. M. McClendon, Dr. C. Madden and Dr. M. Shakouri for providing the heterodyne measurements and for the optical receivers.

References

- [1] C. A. Burrus, J. E. Bowers, and R. S. Tucker, "Improved very-high-speed packaged InGaAs p-i-n punch-through photodiode", *Electron. Lett.*, vol. 21, pp. 262-263, 1985.

- [2] Satoki Kawanishi, Atsushi Takada, and Masatoshi Saruwatari, "Wide-band frequency-response measurement of optical receivers using optical heterodyne detection", *J. Lightwave Technol.*, vol. 7, No. 1, pp. 92-98, 1989.

- [3] Elliot Eichen, John Schlafer, William Rideout, and John McCabe, "Wide-bandwidth receiver/photodetector frequency response measurements using amplified spontaneous emission from a semiconductor optical amplifier", *J. Lightwave Technol.*, vol. 8, No. 6, pp. 912-916, 1990.

- [4] William Rideout, Elliot Eichen, John Schlafer, Joanne Lacourse, and Ed Meland, "Relative intensity noise in semiconductor optical amplifiers", *IEEE Photon. Technol. Lett.*, vol. 1, No. 12, pp. 438-440, 1989.

- [5] K. J. Williams, and R. D. Esman, "Observation of photodetector nonlinearities", *Electron. Lett.*, vol. 28, pp. 731-732, 1992.

- [6] N. A. Olsson, "Lightwave systems with optical amplifiers", *J. Lightwave Technol.*, vol. 7, No. 7, pp. 1071-1082, 1989.

Figure Captions

Figure 1. Reduction in measured photoreceiver responsivity due to finite optical filter bandwidth. Inset shows superfluorescent source with post filtering to increase the relative intensity noise at the receiver.

Figure 2. Frequency response measurements of a 3 GHz receiver performed with: (a) optical heterodyne method; (b) filtered intensity noise technique with $B_o = 1$ nm.

Figure 3. Experimental setup for measurements with etalon filtered intensity noise technique. $F = 80$ and $FSR = 680$ MHz.

Figure 4. Frequency response measurement of a high-speed optoelectronic receiver using (A) unfiltered intensity noise technique (B), filtered intensity noise technique (C) optical heterodyne measurement shown with circles.

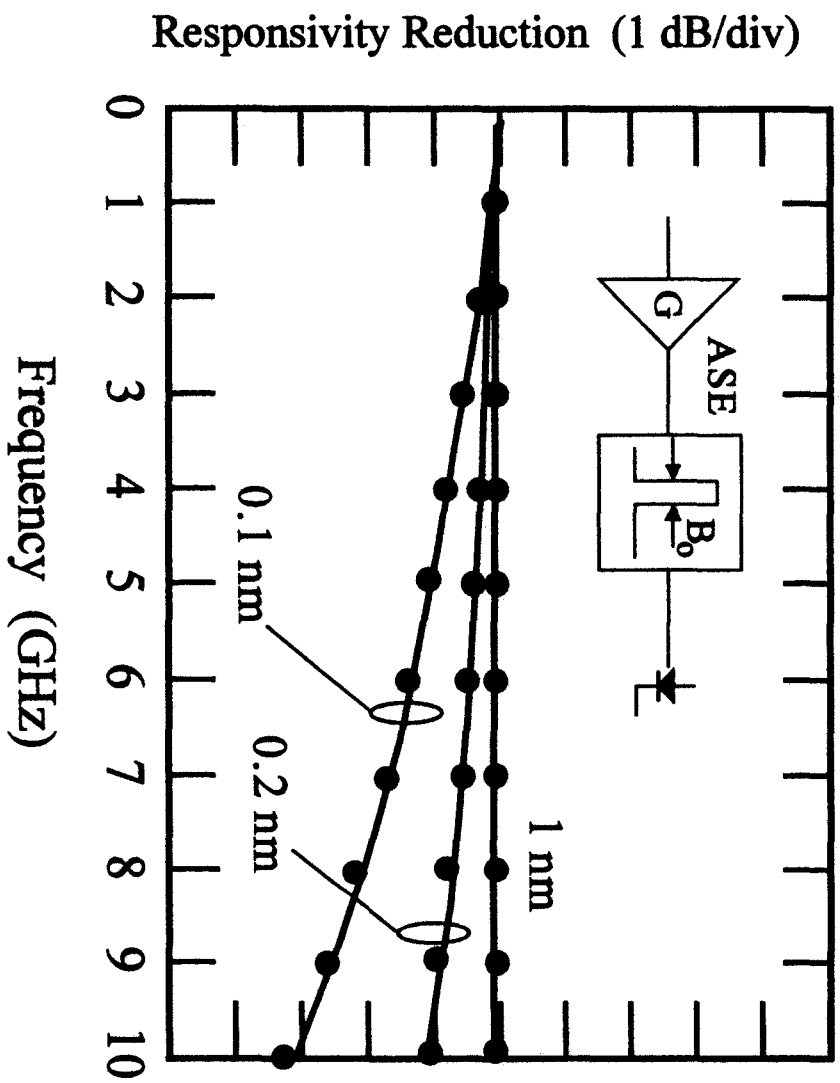


Figure 1

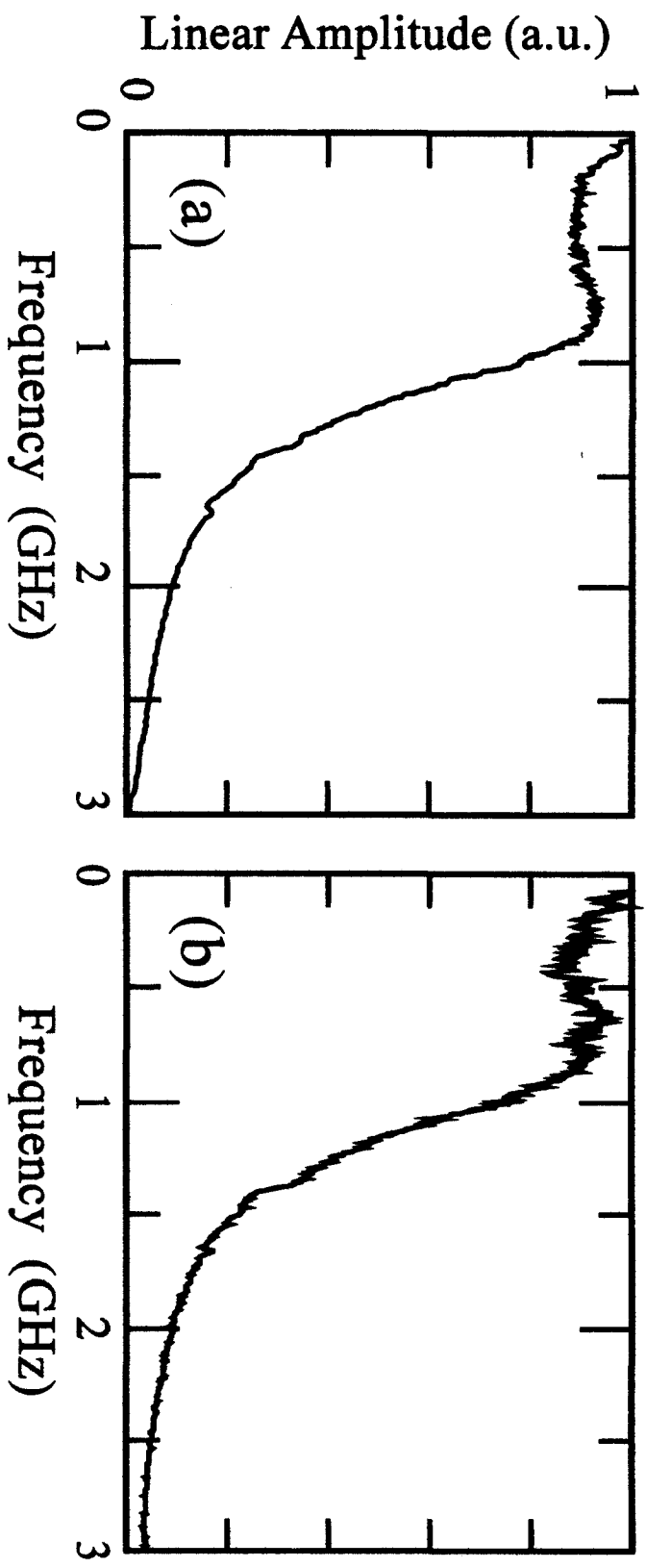


Figure 2

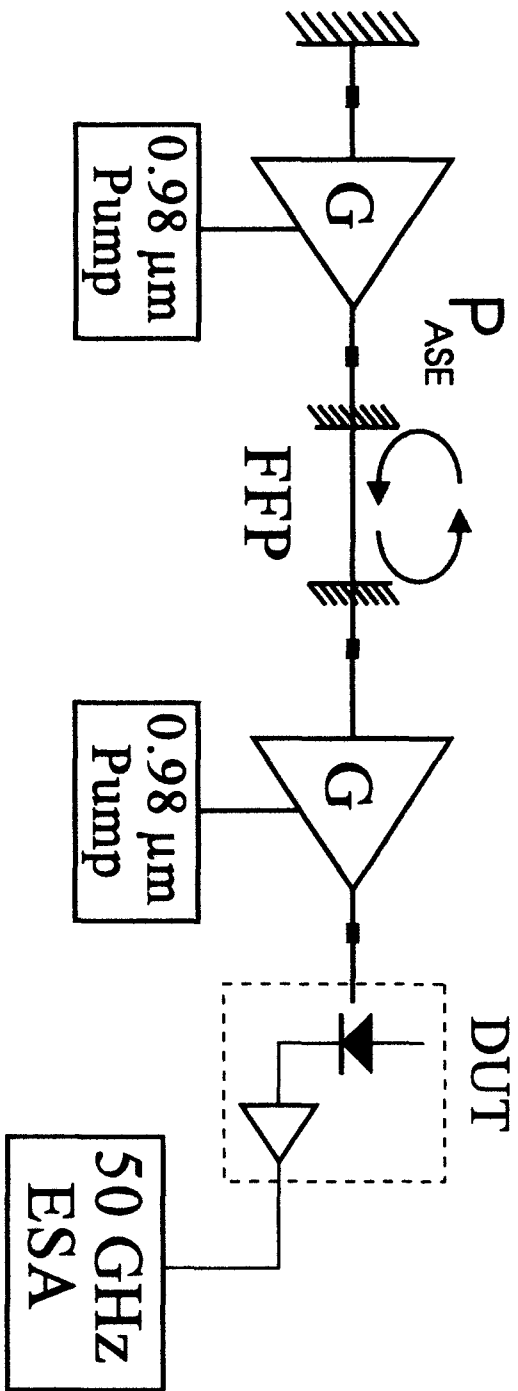


Figure 3

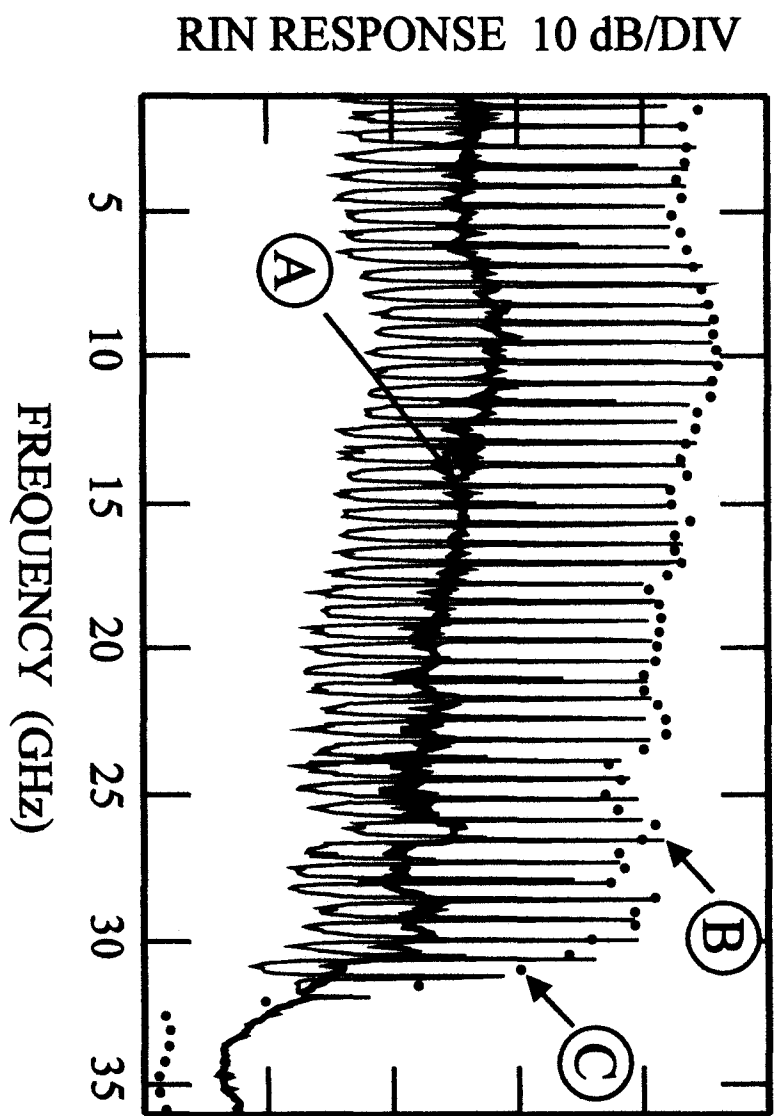


FIGURE 4